

1 **UVC-based air disinfection system for rapid inactivation of SARS-** 2 **CoV-2 present in the air**

3 **Authors:** Harry Garg^{1#*}, Rajesh P. Ringe^{2#*}, Supankar Das¹, Suraj Parkash¹, Bhuwaneshwar
4 Thakur², Rathina Delipan², Ajay Kumar¹, Kishor Kulkarni³, Kanika Bansal², Prabhu B. Patil²,
5 Tabish Alam³, Nagesh Babu Balam³, Chandan Swaroop Meena³, Krishan Gopal Thakur², Ashok
6 Kumar^{3*}, Ashwani Kumar²

7 ¹ Central Scientific Instruments Organisation, Council of Scientific and Industrial Research (CSIR), Sector
8 39-A, Chandigarh, India

9 ² Institute of Microbial Technology, Council of Scientific and Industrial Research (CSIR), Sector 39-A,
10 Chandigarh, India

11 ³ Central Building Research Institute, Council of Scientific and Industrial Research (CSIR), Roorkee,
12 Uttarakhand, India

13
14 # Contributed equally

15 * Corresponding authors: Harry Garg (harry.garg@csio.res.in), Rajesh P. Ringe
16 (rajeshringe@imtech.res.in), Ashok Kumar (ashokkumar@cbri.res.in)

17 **Correspondence:**

18 Rajesh P. Ringe
19 Virology Unit
20 CSIR-Institute of Microbial Technology
21 Chandigarh – 160036, INDIA
22 Email: rajeshringe@imtech.res.in
23 Phone: +91-172-2880163

24
25 **Running title:** UV-C-based disinfection system to inactivate SARS-CoV-2

26 **Keywords:** SARS-CoV-2, UV-C, disinfection, COVID-19, aerosols

27 **Abstract:** The novel coronavirus disease 2019 (COVID-19) infections have rapidly spread
28 throughout the world, and the virus has acquired an ability to spread via aerosols even at long
29 distances. Hand washing, face-masking, and social distancing are the primary preventive measures
30 against infections. With mounting scientific evidence, World Health Organisation (WHO) declared
31 COVID-19 an air-borne disease. This ensued the need to disinfect air to reduce the transmission.
32 Ultraviolet C (UVC) comprising the light radiation of 200-280 nm range is a commonly used method
33 for inactivation of pathogens. The heating, ventilation, and air conditioning (HVAC) systems are not
34 beneficial in closed spaces due to poor or no ability to damage circulating viruses. Therefore,
35 standard infection-prevention practices coupled with a strategy to reduce infectious viral load in air
36 substantially might be helpful in reducing virus transmissibility. In this study, we implemented UV
37 light-based strategies to combat COVID-19 and future pandemics. We tested various disinfection
38 protocols by using UVC-based air purification systems and currently installed such a system in
39 workspaces, rushed out places, hospitals and healthcare facilities for surface, air, and water
40 disinfection. In this study, we designed a prototype device to test the dose of UVC required to
41 inactivate SARS-CoV-2 in aerosols and demonstrate that the radiation rapidly destroys the virus in
42 aerosols. The UVC treatment renders the virus non-infectious due to chemical modification of
43 nucleic acid. We also demonstrate that UVC treatment alters the Spike protein conformation that
44 may further affect the infectivity of the virus. We show by using a mathematical model based on the
45 experimental data that UVC-based air disinfection strategy can substantially reduce the risk of virus
46 transmission. The systematic treatment by UVC of air in the closed spaces via ventilation systems
47 could be helpful in reducing the active viral load in the air.

48

49

50

51

52

53

54

55 **Introduction:** The Severe Acute Respiratory Syndrome Coronavirus-2 (SARS-CoV-2) is
56 responsible for the current pandemic causing millions of infections worldwide and over 2.6 million
57 deaths due to COVID-19 (1). Apart from taking such an enormous toll on human life, the pandemic
58 has imposed unprecedented economic, societal, and healthcare burdens. While mass vaccination
59 drives across the globe are helping to bring back normalcy, there is an urgent need to prevent the
60 virus transmission through aerosols to curb the air-borne transmission to allow the opening of public
61 places and transport such as schools, cinema halls, buses, trains, etc. (2). The attempts to resume the
62 schools, relatively tightly packed and crowded offices, without adequate measures to prevent virus
63 transmission are prime reasons for continued outbreaks (3).

64 Many methods are being explored for the effective disinfection of materials and common-touch
65 surfaces, such as alcohol-based disinfectants, copper surfaces, and soaps. However, there is no
66 effective and safe method that can be deployed in closed workplaces to inactivate the SARS-CoV-2
67 virus in the air. The face masks are particularly effective in restricting transmission through aerosols
68 and prevent the spread (4). However, the common breach in face-mask practices is causing
69 transmission of the virus within small groups and bigger gatherings. UV radiation is known to
70 effectively kill bacteria and viruses (5) and recent studies have shown that this method is effective
71 in inactivating SARS-CoV-2 virus(6). The UV light causes the formation of pyrimidine dimers in
72 the genetic material and inhibits transcription and replication(7). Therefore, the targeted damage of
73 the essential component of the microbes could be an excellent strategy to attenuate the infectivity of
74 viruses, especially the ones which transmit rapidly, such as SARS-CoV-2.

75 The WHO declared in May 2021 that SARS-CoV-2 transmission is not only by common touch, close
76 contact but also through air. Indeed, SARS-CoV-2 was detected in our studies in air samples near
77 hospitals even earlier (8). The air-born transmission has serious implications on the control measures
78 we can deploy in place and emphasizes the reduction of viral load in air. In this study, we explore
79 the UV radiation for its ability to inactivate SARS-CoV-2 present in the aerosols. We study the
80 inactivation kinetics by using different dosages of UV to identify the dosage required to achieve
81 maximum virus inactivation. Devices using UV-C light for sanitization of air within air-ducts of
82 HVAC systems and circulating units for use within occupied spaces were designed, developed and
83 validated for delivering the relevant viricidal doses of UV-C light to the air and maintaining the air
84 change rates required by the ventilation guidelines. Further, a risk assessment model to quantize the

85 risk reduction was developed and implemented where it was found that the use of UV –C light
86 irradiation to sanitize air can result in the reduction of the risk of infection in the occupied spaces by
87 up to 90%.

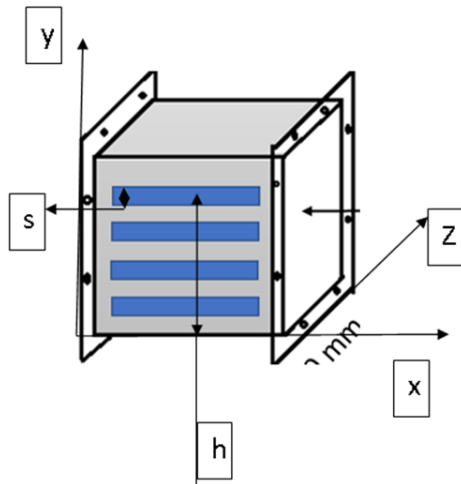
88 **Results:**

89 **Design of ultraviolet C (UVC) Disinfection system:**

90 Based on the market requirements, two types of systems were used – i) in-duct UVC disinfection system and
91 ii) standalone air circulating UV-C disinfection system. These designs are described below.

92 **In-duct UVC disinfection system**

93 In-duct UV systems work for the purpose of inactivating microbes in airstream in a building or zonal
94 ventilation system. The UV lamp is key component and the design and optimization of in-duct UV
95 systems revolves around various features of it. The in-duct system also depends on the output
96 characterization, required UV dose for microbicidal activity, and energy consumption evaluations
97 of UV systems. The in-duct system we designed consisted of UV lamps, fixtures, and ballasts. In
98 the chamber, the access to the air by UV radiation is uniform and so the UV lamps could be fixed at
99 any location including air handling unit (AHU) (**Figure 1**). While designing the systems, we placed
100 the lamp fixtures and ballasts either internally or external to the ductwork. The drop in pressure with
101 external fitting was relatively less than internal fitting. In any case, the drop in pressure associated
102 with UV radiation was only marginal when the velocity of air was within the normal limits of 2–3
103 m/s (400–600 fpm). By applying these parameters, the modular systems were made and installed in
104 ductwork. The UV radiation may not disinfect the air in one encounter but recirculation of air from
105 the room via the system will increase such encounters and give multiple UV doses to airborne
106 microorganisms for maximum disinfection. Therefore, the re-circulation systems are more efficient
107 than single-pass systems in which air is not recirculated. The characteristics of an air stream that can
108 impact the design are relative humidity (RH), temperature, and air velocity. However, air
109 temperature has a negligible impact on microbial susceptibility in general although membrane
110 viruses such as coronavirus are more susceptible to higher temperature because of rapid drying of
111 aerosols in the hotter environments. The RH factor is compensated as the UV systems are installed
112 after the conditioned air and before the delivery in user place.

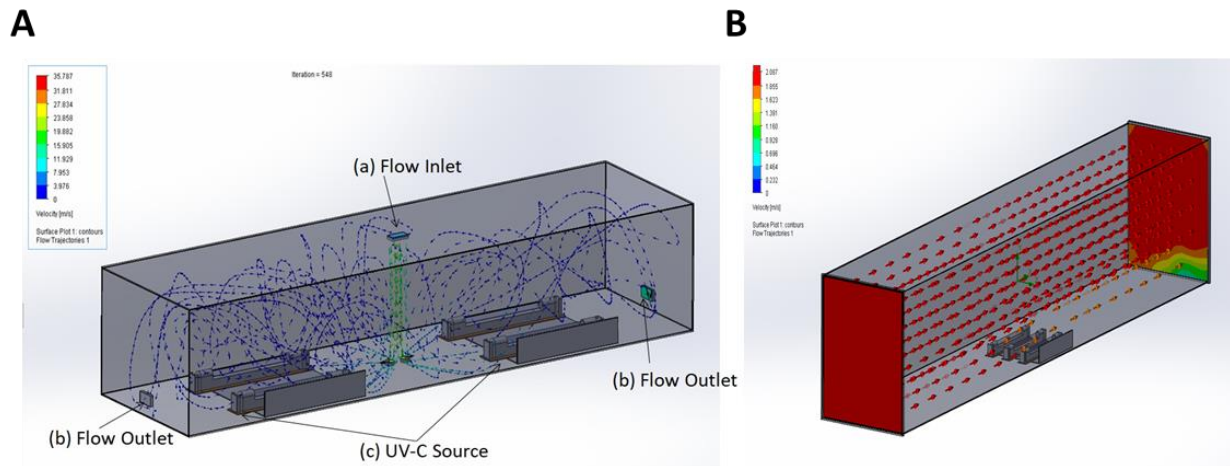


113
114 **Figure 1:** Configuration of induct UV-C disinfection system. Induct UV-C air disinfection system
115 in a cartesian coordinate system with flow in x direction, Illumination in z-direction and source
116 installation in y-direction. The scale is in mm.

117 In addition to this, duct disinfection system depends upon following parameters i) duct dimensions
118 ii) duct materials iii) air temperature iv) amount of recirculated air v) amount of fresh air in
119 recirculation, and vi) flow rate. The different parameters of the proposed systems were X: Length of
120 the source in X-axis, Y: height of the source surface in Y-axis, Z: target surface in Z-axis, and h:
121 total installation height. The UV intensity was evaluated from these parameters considering the flow
122 rate. The required parameters such as flow rate, exposure time, no of air changes, installation space,
123 and UV intensity were optimized to get the required dosages for deactivation of the virus and
124 maintain the constant fluence rate in the duct. The design of the induct UV-C system (unidirectional
125 or bi-directional) is shown in [Figure 2](#). It shows an enclosed space with source to target illumination
126 surface in z direction and the system was used in the closed indoor space.

127 The principal design objective for an in-duct UV-C air disinfection system is to create UV energy
128 distribution uniformly throughout a specified length of the duct or air-handling unit (AHU) to deliver
129 the appropriate UV dose to bacteria/virus/aerosol particle in the air moving through the irradiated
130 zone with minimum system power as shown in [figure 3](#). Enhancing the overall reflectivity of the
131 inside of the air handler or air duct improved UV-C system performance by reflecting UV-C energy
132 back into the irradiated zone, thus increasing the effective UV dose and maintain the constant fluency

133 rate. The flow rate was optimized and the change in air flow rate due to the obstruction of the UV

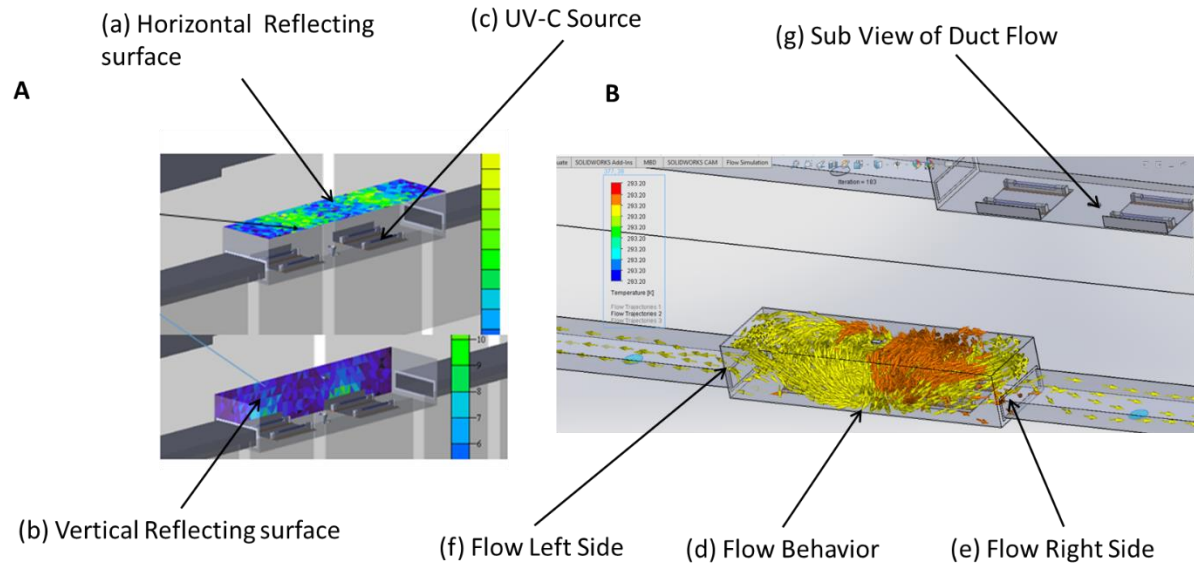


134
135 **Figure 2:** Large size duct with UV-C air disinfection system A) bi-directional flow system with (a) flow inlet
136 at top as infected/recirculated air enters, treated in the duct within volumetric space and disinfected delivery
137 of air exhaust (b) left and right side and (c) UV source fixtures. The blue dotted lines show the flow trajectory
138 of air. B) unidirectional flow system with the UVC source at bottom and air being treated in disinfection
139 volume using. The scale shows the velocity in m/s

140 source in the flow was evaluated, which was negligible in the design. The designed and fabricated
141 duct is shown in [figure 4](#).

142 1.1 Standalone recirculation Air disinfection:

143
144 The recirculation UV disinfection systems were installed in the smaller workplaces, each consisted
145 of UV lamps and fixtures in a housing containing a blower. The airflow in recirculation units were
146 in the range of 1.4–14 m³/min (50–500 cfm) and were suitable for small rooms or apartments only.
147 Many recirculation units were portable and could be positioned on the floor, tables, mounted on wall
148 or ceiling. Room recirculation units and upper air systems were installed to augment in-duct systems
149 or where in-duct installation was not feasible. The prototype stand-alone unit was tested under
150 laboratory condition and based on the results these units are currently installed for application in the
151 real-world scenario. Due to requirements of compact size, the internal volume of recirculation units
152 do not usually allow extended exposure times to deliver the viricidal dosages during the transit of
153 air through them. Hence, the units were carefully designed to create enough serpentine paths



154
155 **Figure 3:** Disinfection of air in flow ducts considering irradiance plot and flow behavior A) The irradiance
156 plot of duct on target surface in horizontal (a), vertical surface (b), and UVC source (c). B) bidirectional flow
157 behavior of air from the center of duct.

158 through the circulating devices within the volume irradiated by the UV –C light so as to deliver the
159 viricidal dosages while the units remained compact and portable. The air that goes into the unit
160 comes out sanitized to the extent of over 99% of the virus load reduction.

161 Both the in-duct and the standalone systems were designed for applications ranging from very small
162 volume and low flow rate to high volumes and high flow rates for different applications such as lifts,
163 toilets, classrooms, workspaces, offices, meeting halls and auditorium etc. The details of the different
164 systems are as shown in [table 1](#).

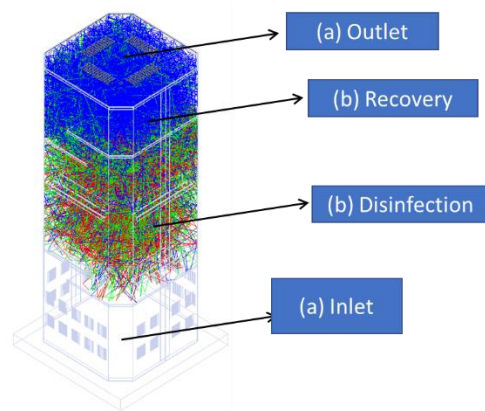
165 **Design of a standalone system to measure the effect of UVC on SAS-CoV-2 survival in air**

166 A hermetically sealed chamber was designed to study the dosage of UVC required to inactivate
167 SARS-CoV-2 present in aerosols. The volume of the aerosol generation and the volume of the UV
168 treatment are interrelated. The aerosols were created from virus suspension by using the nebulizer
169 which produces mist by creating low-pressure zone at the surface of the liquid which pulls up fine
170 droplets from the liquid surface. The shape of the chamber was designed to be a rectangular with the
171 dimension of 56x41x31 cm to ensure the uniform distribution of aerosols ([Figure 5B and 6B](#)). The

172 Table 1: Types of UV-C disinfection systems

S. No	Parameters	In-duct UV-C disinfection systems for HVAC buildings	In-duct UV-C disinfection systems for HVAC buses	Standalone UV-C disinfection system
i.	Flow rate (CFM)	>30,000	<3000	<300
ii.	Applicable space(ft ²)	>1000	<350(customizable)	<150
iii.	Shape and size	Rectangular >300mm	Rectangular <300mm	Rectangular <1500mm
iv.	Wattage(W)	>100	<100	<70
v.	Weight	<2.5 Kg	<1.2 Kg	<3.0 Kg
vi.	UV source(nm)	254	254	254
vii.	Length of the delivery duct(m)	>10	<2	<0.5
viii.	Exposure time (sec)	1.1	1.14	1.1
ix.	Dosages	>1.6mJ/cm ²	>1.3mJ/cm ²	>1.3mJ/cm ²

173



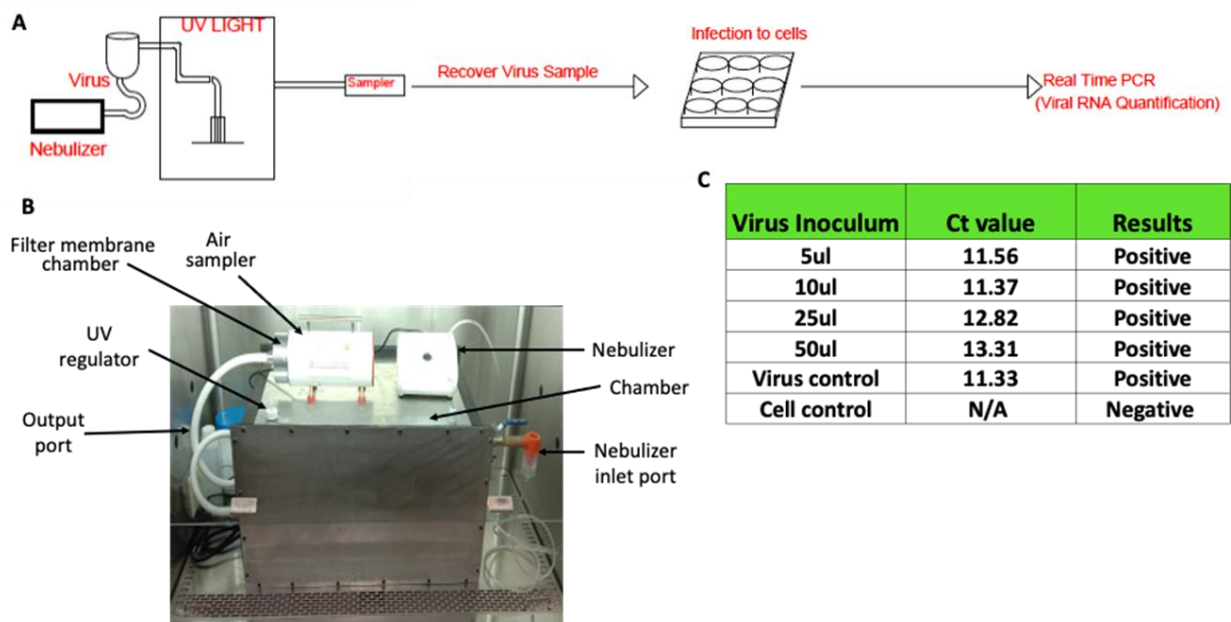
174

175 **Figure 4: Standalone Air disinfection system with flow in vertical direction.** Shown is the inlet for air (a),
 176 UVC treatment compartment (b), the recovery area (c), and outlet for the disinfected air (d).

177 inlet and outlet of the chamber were customized to fit to the nebulizer pipe and sample collection
 178 tube respectively. The regulator was installed to control the UV-C intensity. The air filtration unit
 179 was connected to the chamber to suction the air from the chamber and a filter was placed in the outlet
 180 pipe to collect the aerosols on the surface of the filter membrane.

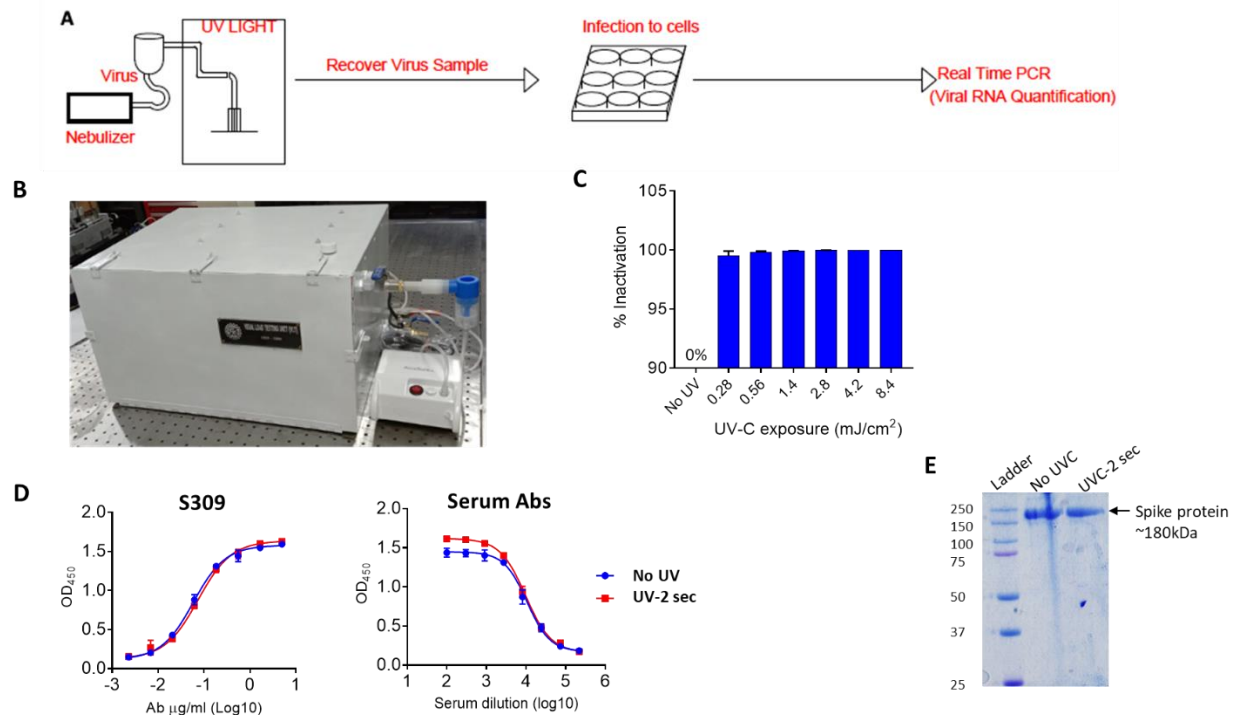
181 **Testing the efficiency of Induct UVC air disinfection system against aerosolized SARS-CoV-2:**

182 A number of different methods are used to entrap the airborne viruses. These include impactors,
183 electrostatic precipitators, filters, etc. (9). The transmission of COVID-19 has been primarily
184 estimated through collecting specified volumes of air on filters followed by estimation of viral load
185 through quantitative real-time polymerase chain reaction (qRT-PCR) (10, 11). However, such
186 methods only look at the presence of virus particles in the air samples which does not provide any
187 information on infectious dose. Since our primary goal was to evaluate the effect of UV radiation on
188 the infectivity of air borne SARS-CoV-2, we designed an air sampling chamber as described above
189 to entrap air-borne SARS-CoV-2 and assess the infectivity after UV irradiation (design of device
190 and experimental set-up is shown in [Figure 5A](#) and actual device is shown in [Figure 5B](#)). For each
191 cycle of aerosol generation, virus suspension containing 1.5×10^7 pfu was nebulized into the



192
193 **Figure 5: Workflow of SARS-CoV-2 aerosol generation and detection of virus in air.** A) The schematic
194 of aerosol generation, virus sampling, infection and detection of virus growth B) The UVC treatment and air
195 sampling device C) The effect of gelatin on the viability of SARS-CoV-2. The virus supernatant was applied
196 onto gelatin membrane and recovered by dissolving membrane in PBS to assess infectivity in Vero-
197 TMPRSS2 cells. The Ct values for original virus supernatant (virus control) and gelatin-recovered virus are
198 indicated in the table.

199 chamber. Two minutes were sufficient to produce aerosols from approximately 90% of the loaded
200 virus stock in the nebulizer. The nebulized SARS-CoV-2 was either collected directly (control) or
201 exposed to UV light and then collected by trapping them onto a gelatin filter using an air sampling
202 device that channeled the air through a gelatin filter (Figure 5B). The filtration unit was turned on
203 with the speed of 100 L/min of air to collect virus particles on the filter. The gelatin filter was
204 solubilized in DMEM and then used to infect Vero-E6-TMPRSS2 cells in a 48-well plate, each well
205 containing 4×10^4 cells. The Vero-E6-TMPRSS2 expresses a moderate level of ACE-2 but high
206 TMPRSS2, which has been shown to have increased SARS-CoV-2 infectivity by 100-folds(12). The
207 infection by collected sample from the membrane was performed for 75 minutes, after which cells
208 were washed, and grown in fresh growth medium supplemented with 5% FBS for 48-hours. Virus
209 particles were quantified by examining the viral RNA in culture media. After 48 hours of infection,
210 the viral RNA was not detected in control as well as UV-treated samples. To test whether gelatin
211 had any virus inhibitory property, virus suspension (10^6 pfu/ml stock) was directly added to the



212
213 **Figure 6:** Inactivation of SARS-CoV-2 present in air: A) The schematic of aerosol generation virus sampling,
214 infection and detection of virus growth B) The stand-alone UVC-based device without the air sampling
215 connector to sample air containing aerosolized virus inside the chamber. C) Inactivation of SARS-CoV-2 by
216 UV treatment. The recovered virus aerosols from quartz tube after UV treatment were resuspended in growth
217 medium and used for infection of Vero-TMPRSS2 cells for 48 hours. Cell supernatants were analysed for

218 viral RNA. Percent inactivation of virus at various UV-C exposures with reference to no UV treatment was
219 recorded. D) The binding of S309 or serum antibodies to spike protein is shown in dose-dependent manner.
220 E) The spike protein with or without UVC treatment in SDS-PAGE.

221 gelatin filters and incubated for 10 minutes. After incubation membrane was solubilized in DMEM
222 as described above and used for the infection of cells. The viral genomic RNA was detected in the
223 culture supernatants indicating that virus infection and replication took place. replication we were
224 able to culture infectious SARS-CoV-2 (Figure 5C). Collectively, these findings indicate that SARS-
225 CoV-2 viruses are probably quite fragile and susceptible to air-drying and collision onto the solid
226 surfaces.

227 **Testing the efficiency of standalone UVC air disinfection system against SARS-CoV-2 virus:**

228 As mentioned above, the traditional device such as an air sampler was not suitable for the analysis
229 of infectivity of SARS-CoV-2 due to mechanical disruption of virus particle by collision with the
230 filter. Therefore, we aimed to develop a tool wherein we could expose the SARS-CoV-2 to UV and
231 then collect the virus to analyze its infectivity (Figure 6A). We were specifically interested in using
232 UV irradiation for disinfection of SARS-CoV-2 since it has several advantages over existing
233 chemical and conventional disinfectants, such as negligible emergence of resistance, and it does not
234 chemically affect the material. To circumvent the issues related to the trapping of viral particles
235 through an air filtration device, we took inspiration from the natural mode of SARS-CoV-2
236 transmission. The droplet nuclei containing SARS-CoV-2 are usually inhaled by healthy individuals
237 and deposited inside the airway system. To create a new device to monitor the infectivity of viral
238 particles, we utilized aerosol's tendency to settle on the surfaces such as glass and steel to trap the
239 viruses (13). SARS-CoV-2 was nebulized, and then the nebulized particles were released into a
240 quartz tube in an air-tight aerosol chamber connected to the nebulizer (Figure 6B). This device was
241 placed inside a biosafety cabinet to ensure the containment of aerosolized SARS-CoV-2. The device
242 was equipped with a 30 mW UV light tube enabling exposure of the trapped viruses in the center of
243 the device. After UV exposure, the quartz tube was rinsed with cell culture media to recover the
244 viruses. Since we were unable to recover viruses directly by passing aerosolized air through a gelatin
245 filter in the induct UVC disinfection system, here we used quartz tubes to collect the aerosols and
246 then exposed to UV. The open quartz tubes were placed inside the chamber to collect the aerosol
247 sample. The suspension containing 1.5×10^7 pfu virus was aerosolized for two minutes as described
248 above and then exposed to UV light at different doses ranging from 2.8 mJ/cm^2 to 16.8 mJ/cm^2 . UV

249 dosage of 0.28 mJ/cm² was sufficient to inactivate 99.2% SARS-CoV-2 whereas UV dosage of 0.56
250 mJ/cm² resulted in 99.8% inactivation of SAR-CoV-2 (Figure 6C). Thus, we concluded that 0.28
251 mJ/cm² is sufficient to inactivate the aerosolized virus meaningfully. The disinfection of virus is
252 most likely due to chemical modification of genomic RNA but we also investigated whether UVC
253 has any effects on Spike protein of SARS-CoV-2. To this end, we used SARS-CoV-2 spike protein
254 ectodomain (spike-6P) stabilized in pre-fusion state. The UVC irradiation equivalent to 0.28 mJ/cm²
255 enhanced the binding of serum antibodies but not the S309 antibody which recognized the conserved
256 epitope in RBD (Figure 6D). The UVC treatment did not break the peptide chain and only one intact
257 band appeared on SDS-PAGE (Figure 6E). This data suggested that UV radiation alters the
258 conformation of spike protein and may thus affect the entry of the virus. In summary, the above-
259 described observations suggest that UV radiation can efficiently inactivate the air-borne SARS-
260 CoV-2 and it could be used for disinfection of air.

261 **Risk analysis of infection and reduction of risk**

262 The UV-based air disinfection system resulted in rapid loss of infectious SARS-CoV-2 and based
263 on this data we next assessed the reduction of transmission risk when this system is used in real
264 world scenario. Transmission of pathogenic microorganisms is a complicated process. This
265 comprises pathogen features, the number of particles produced in a potentially pathogenic host, how
266 effectively the pathogen survives or remains viable outside that host, and the immune system of a
267 person who is exposed to the pathogen. For decades, the Wells-Riley model has been primarily
268 employed for this purpose (14).

$$269 \quad P = 1 - e^{-n}$$

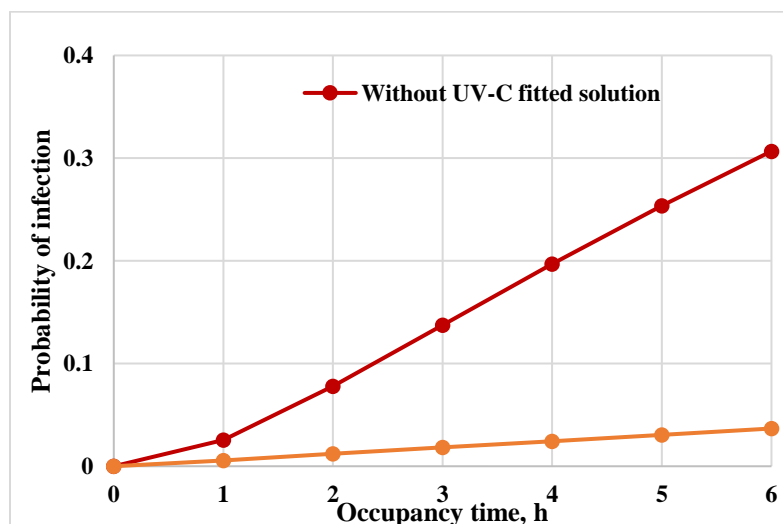
270 Where, P is the probability of infection for susceptible persons and n is the number of quanta inhaled.
271 The quanta inhaled is influenced by the average quanta concentration (C_{avg} , quanta/m³), volumetric
272 breathing rate of an occupant (Q_b , m³/h), and the duration of the occupancy (D,h).

$$273 \quad n = C_{\text{avg}}Q_bD$$

274 The airborne quanta concentration rises with time from zero to one minus exponential. The time
275 dependent airborne concentration of infection quanta depends on loss rate coefficients which is a
276 sum of ventilation rate, deposition on to surfaces, virus decay and filtration or air disinfection
277 efficiency(15).

278 To quantify the impact of the virus concentrations, we considered an example of a secondary school
279 class room which consists of 40 students and a faculty. Let us consider faculty is infected with
280 SARS-CoV-2 assuming no susceptible student is wearing mask and are un-vaccinated. The
281 breathing rate of the faculty as per the taking activity is 1.1 (15) and the quanta emission rates for
282 this activity as 9.7 (16). The recommended rate of air circulation for school building is 5 air changes
283 per hours (17). The surface deposition loss rate considered as 0.3 (1/h) (18, 19). Fears et al. (20)
284 observed no virus decay in virus-containing aerosol for 16 hours at 53% relative humidity, but van
285 Doremalen et al. (13) calculated the half-life of airborne SARS-CoV-2 to be 1.1 h, corresponding to
286 a decay rate $k = \ln(2)/t_{1/2}$ of 0.63 1/h.

287 As per the investigation the efficiency of the UV dosage of 0.28 mJ/cm^2 leads to a 99.2%
288 while UV dosage exposure of 0.56 mJ/cm^2 resulted in 99.8% inactivation of SAR-CoV-2. Consider
289 the UV-C disinfection system efficiency as 99.5% as an average of two, the risk of infection and



290
291 **Figure 7:** The mathematical model of the risk reduction by UV-C treatment of air. Based on the results of
292 SARS-CoV-2 virus inactivation using stand-alone device the risk reduction in the class room was modelled.
293 Shown is the % reduction of risk with the function of exposure time.

294 reduction in risk calculation for class room with 6 hours of operation is presented in Figure 9.
295 Without UV disinfection, after 6 hours of occupancy in the classroom, 13 students out of 40 could
296 become infected with SARS-CoV-2 (Figure 7). In comparison, after implementing a UV
297 disinfection solution, the risk of infection is reduced by 90%.

298

299 **Materials and Methods:**

300 **Design of UV Disinfection system:**

301 Both the systems are developed using commercial bill of material (BOM). Certified UVC sources,
302 Aluminum plates with surface treatment, commercial grade fasteners and fittings were used. The
303 UV lamps used in the system were of 254nm wavelength and were obtained from commercial
304 source. The qualified power supplies, Teflon wiring with extra sleeves was used as safety measure.
305 The developed system also met all the commercial safety, environmental and electromagnetic
306 induction (EMI) directives. The systems were robust in design and had satisfactory performance to
307 inactivate coronavirus at the installed places. All the parameters considered for designing the system
308 are listed in table 1.

309 Both the induct UVC air disinfection system and the standalone air disinfection system are designed
310 according to the required optimum dosages, flow rates and the duct dimensions. The system was
311 designed in such a way that it does not affect the flow rates through the delivery duct and the UVC
312 systems were mounted along the side wall in induct UVC air disinfection system. The Induct system
313 comes in two configurations i.e extraction & retraction type mechanism (refer figure 1 & 2) for the
314 overhead delivery ducts and the fixed type (refer figure 2 and 4) for the separated delivery ducts.
315 The standalone system (figure 5) is used in public places with the human life and has a fixed UVC
316 sources and is designed to meet the standard COVID ventilation guidelines and 10 ACH (air changes
317 per hour). Both the systems were adequately sealed and UV leakage protection was ensured through
318 the optimum sealing. In order to increase the effectiveness of the UVC source, the aluminum
319 polished plates were used and the irradiated zone had high finish aluminum surface for efficient
320 delivery.

321 **SARS-CoV-2 virus preparation:** All the experiments involving the handling of the SARS-CoV-2
322 virus were performed in the BSL3 facility at CSIR-Institute of Microbial Technology, Chandigarh,
323 according to the institutional biosafety guidelines (IBSC approval no
324 CSIR/IMTECH/IBSC/2020/J23) and institutional ethics guidelines (IEC May 2020#2). The SARS-
325 CoV-2 strain used in the study was isolated from an Indian patient and cultured using the VeroE6
326 cell line as per the established methods (21, 22). The SARS-CoV-2 was confirmed by whole-genome
327 sequencing and the sequence was submitted to gene bank (Accession # EPI_ISL_11450498). An

328 aliquot of the virus from passage-1 was used to inoculate the 25mm cell culture flask containing
329 Vero E6 cells with 80-90% confluent cells in 5 mL medium. The virus growth was monitored
330 regularly. After extensive cytopathic effect, virus suspension was harvested, clarified and aliquoted
331 in microcentrifuge tubes for long storage at -80°C until further use. The viral load was estimated by
332 quantitative real-time PCR (GCC Biotech) by using 10 µl sample diluted in 100 µl growth medium.
333 Same virus stock was used for all the experiments.

334 **Aerosol generation, sample collection and infection of cells by aerosol samples:** Before setting
335 up the experiments, the device was cleaned and disinfected using 70% ethanol. The working 0.5mL
336 virus stock was freshly thawed for aerosolization. The sterile quartz tube was placed inside the UV
337 chamber and the chamber was closed from all sides. 0.5 mL virus solution was loaded in the sample
338 holding cup of the nebulizer and the mouthpiece was then attached to the inlet tube of the UV device.
339 The aerosols were created and allowed to accumulate in the device chamber for 2 minutes. UV
340 irradiation was done for the required period of time by using a UV light switch outside the bio-safety
341 cabinet. After UV treatment, the quartz tube was removed carefully from the UV chamber, and
342 immediately 0.5mL growth media was added to rinse the surface of the tube. 50 µL sample was then
343 used to infect the cells in a 48-well tissue culture plate containing 5×10^4 Vero-E6-TMPRSS2
344 (JCRB1819) cells per well(12). The infection was done for 1 hour with intermittent swirling. After
345 incubation, cells were washed with 200 µL sterile PBS, and a fresh 200 µL growth medium was
346 added to the wells, and the plate was further incubated for 24 hours at 37°C in the atmosphere of 5%
347 CO₂.

348 **Quantitative real-time PCR (qRT-PCR): The Vero cell supernatants were harvested from the**
349 **test plate after required incubation.** RNA was isolated from 140ul supernatant for qRT-PCR-
350 based analysis. The RNA isolation by Qiagen RNA isolation kit and qRT-PCR by GCC Biotech was
351 performed by using the manufacturer's instructions. The qRT-PCR was performed by using Bio-
352 Rad system CFX96 Real-Time System. The extent of virus inactivation was calculated by
353 quantifying viral RNA in respective virus cultures from UV-treated aerosols and non-treated
354 aerosols.

355 **SARS-CoV-2 spike protein expression:** expi293 cells were cultured in 30ml Erlenmeyer flasks in
356 freestyle expression media in humidified incubator with 5% CO₂ at 37°C temperature. The shaking
357 speed was 130rpm/min. The cells were seeded 1 day before transfection to achieve 3×10^6 cells/ml

358 at the time of transfection. The cells were transfected by using polyethyleneimine (PEI) transfection
359 reagent (Polysciences). Transfected cells were further incubated at constant shaking speed for 4 days
360 before harvesting the culture supernatant. The supernatant was filtered through 0.45µ filters and
361 passed slowly through HisPur Ni-NTA resin column (ThermoFisher Scientific) with the speed of
362 ~0.1 ml/minute. The nickel beads were washed twice with washing buffer (NaCl) followed by
363 elution with Imidazole (150mM). The eluate was then dialyzed overnight in PBS and protein was
364 concentrated by using Amicon Pro centrifugal filter (Millipore). The protein was quantified by using
365 BCA Protein Assay Kit (ThermoFisher Scientific).

366 **SDS-PAGE:** 2µg protein was loaded on 10% SDS-gel followed by staining with Coomassie brilliant
367 blue dye.

368 **Enzyme-linked Immunosorbent Assay (ELISA):** 1µg/ml spike protein in PBS was coated
369 overnight in 96-well plate followed by washing and blocking the plate with PBS containing 5% FBS
370 plus 1% skimmed milk for 1 hour. After blocking, S309 or vaccine serum was added in serial dilution
371 and incubated for 2 hours at room temperature. The antibodies were washed thrice using PBS and
372 anti-human secondary antibody diluted as 1:3000 was added for 1 hour. The plate was washed four
373 times with PBS containing 0.1% tween20 followed by addition of TMB substrate. The reaction was
374 stopped by adding 0.3M H₂SO₄. The optical density was recorded by reading the plate at 450nm.

375 **Discussion**

376 In this study, we have explored the effectiveness of UV light to inactivate the SARS-CoV-2 virion
377 particles present in aerosols. UV radiation is long known to be sterilizing agent for microbes in the
378 laboratories, hospitals, and food industry and is regularly used to sterilize various materials. Unlike
379 bacterial, parasitic, or fungal pathogens, viruses has small genetic material with a simpler physical
380 structure and thus are more susceptible for UV-induced destruction(5). UV-C is considered to be the
381 most effective band of the UV spectrum and efficiently catalyzes the formation of photoproducts in
382 DNA(23). Thymidine dimers irreversibly interrupt essential process of replication, transcription, and
383 translation culminating into the inability of virus particle to establish infection. This study
384 demonstrate that UV-C rapidly inactivates the SARS-CoV-2 virions present in the air.

385 SARS-CoV-2 is highly infectious virus which is evident from rapid spread of this virus from close
386 or continuous contact with the infected person or from common touch surfaces. Our study using the

387 air sampler, however, revealed that virus in the aerosols is quite sensitive to physical collision of the
388 aerosols onto the solid surface and desiccation. Both these factors could be affecting the membrane
389 integrity or Spike protein structure which has likely accounted for the virus inactivation. The results
390 suggest that strong air current might help virus inactivation in the air and UV-C would further reduce
391 the viral load to non-infectious baseline.

392 In 2020, when world witnessed huge COVID-19 infections and death toll, there were no vaccines
393 and effective anti-viral drugs available. Upon the onset of vaccines in 2021, we are poised to have
394 better control over the pandemic and are in far better condition to prevent the new infections or
395 disease severity. However, new studies reveal that the vaccine-mediated immunity wanes over time
396 and increases the chance of re-infection(24, 25). Moreover, the elderly and immunocompromised
397 people are more susceptible to re-infections even after vaccination. Getting back to the normal life
398 is important for the sustainability and will require effective method to inactivate the SARS-CoV-2
399 from our surrounding to prevent the chances of infection. As SARS-CoV-2 is air-borne and highly
400 infectious rapid and effective air sterilization could substantially contribute to reduce viral load in
401 air. In addition, the pathogens are not likely to acquire any resistance to this sort of mechanical
402 inactivation. Our study reveals that UV-C radiation effectively inactivates SARS-CoV-2 in highly
403 concentrated virus-loaded aerosols in the air. The exposure to the UVC radiation equivalent to 0.28
404 mJ/cm² is enough to reduce >99% viruses and therefore can be used to devise the strategies of air-
405 purification.

406 In conclusion, the air-disinfection technology based on UV is a promising alternative to implement
407 disinfection protocols in crowded places. The workplaces such as large offices, hospitals, etc are
408 potential settings that are vulnerable for rapid transmission. The UV systems are generally used in
409 combination with HEPA filters which surely enhances the pathogen filtering capacity but also can
410 increase the cost and maintenance of the systems. The viral pathogens especially respiratory viruses
411 could be inactivated by simple UVGI systems. The facile design of our systems presented in this
412 study and the methodologies are accurate for sizing UV systems.

413
414 **Author Contributions:** HG, SD, SP designed and fabricated the UV in-duct systems. KGT, AK,
415 RPR designed experiments related to testing of in-duct systems to inactivate SARS-CoV-2 in
416 aerosols. RPR and BT performed experiments related to SARS-CoV-2 live virus. KB and PBP did

417 whole-genome sequencing of SARS-CoV-2 isolate. KK, Aku (Ashok Kumar), and NBB performed
418 mathematical modelling using experimental data. HG and RR wrote the original draft of the paper
419 with the comments from AK, KK, Aku.

420 **Acknowledgement:**

421 We thank Dr. Shekhar Mande, Dr Ram Vishwakarma, Dr Rakesh Mishra, Dr Anjan Ray, Dr Anantha
422 Ramakrishna, Dr Sanjeev Khosla, Dr. N. Gopalakrishnan and other members of the CSIR Strategy
423 Group (CSG) for COVID for their guidance and advice in conceiving this project. We are grateful
424 to Dr. Hari Om Yadav for coordinating the project on air disinfection systems. We thank Arushi
425 Goel and Nishant Raj Kapoor for technical assistance. This work was funded by grant from Council
426 of Scientific and Industrial Research (CSIR) and Science and Engineering Research Board
427 (IPA/2020/000168 to RPR). RPR is the recipient of DBT-Ramalingaswami fellowship. This is
428 manuscript 035/2022 from CSIR-Institute of Microbial technology.

429 **Declaration of Interests:** The patent on UV-C-based in-duct designs have been filed in India on
430 which HG, SD, SP, SAR, AK, and RPR are the inventors. The patent on air disinfection and
431 purification system for indoor applications has been filed on which NBB, TA, AKu, CSM, KSK,
432 SG, SD are inventors. Other authors declare no competing interests.

433 **References**

- 434 1. **Hu B, Guo H, Zhou P, Shi ZL.** 2021. Characteristics of SARS-CoV-2 and COVID-19. *Nat Rev Microbiol*
435 **19**:141-154.
- 436 2. **Goralnick E, Kaufmann C, Gawande AA.** 2021. Mass-Vaccination Sites - An Essential Innovation to
437 Curb the Covid-19 Pandemic. *N Engl J Med* **384**:e67.
- 438 3. **Theuring S, Thielecke M, van Loon W, Hommes F, Hulso C, von der Haar A, Korner J, Schmidt M,**
439 **Bohringer F, Mall MA, Rosen A, von Kalle C, Kirchberger V, Kurth T, Seybold J, Mockenhaupt FP,**
440 **Group BS.** 2021. SARS-CoV-2 infection and transmission in school settings during the second COVID-
441 19 wave: a cross-sectional study, Berlin, Germany, November 2020. *Euro Surveill* **26**.
- 442 4. **Brooks JT, Butler JC, Redfield RR.** 2020. Universal Masking to Prevent SARS-CoV-2 Transmission-
443 The Time Is Now. *JAMA* **324**:635-637.
- 444 5. **Hijnen WA, Beerendonk EF, Medema GJ.** 2006. Inactivation credit of UV radiation for viruses,
445 bacteria and protozoan (oo)cysts in water: a review. *Water Res* **40**:3-22.
- 446 6. **Storm N, McKay LGA, Downs SN, Johnson RI, Birru D, de Samber M, Willaert W, Cennini G, Griffiths**
447 **A.** 2020. Rapid and complete inactivation of SARS-CoV-2 by ultraviolet-C irradiation. *Sci Rep*
448 **10**:22421.
- 449 7. **Douki T, Court M, Sauvaigo S, Odin F, Cadet J.** 2000. Formation of the main UV-induced thymine
450 dimeric lesions within isolated and cellular DNA as measured by high performance liquid
451 chromatography-tandem mass spectrometry. *J Biol Chem* **275**:11678-11685.

- 452 8. **Moharir SC, Thota SC, Goel A, Thakur B, Tandel D, Reddy SM, Vodapalli A, Singh Bhalla G, Kumar**
453 **D, Singh Naruka D, Kumar A, Tuli A, Suravaram S, Chander Bingi T, Srinivas M, Mesipogu R, Reddy**
454 **K, Khosla S, Harshan KH, Bharadwaj Tallapaka K, Mishra RK.** 2022. Detection of SARS-CoV-2 in the
455 air in Indian hospitals and houses of COVID-19 patients. *J Aerosol Sci* **164**:106002.
- 456 9. **Verreault D, Moineau S, Duchaine C.** 2008. Methods for sampling of airborne viruses. *Microbiol*
457 *Mol Biol Rev* **72**:413-444.
- 458 10. **Corman VM, Landt O, Kaiser M, Molenkamp R, Meijer A, Chu DK, Bleicker T, Brunink S, Schneider**
459 **J, Schmidt ML, Mulders DG, Haagmans BL, van der Veer B, van den Brink S, Wijsman L, Goderski**
460 **G, Romette JL, Ellis J, Zambon M, Peiris M, Goossens H, Reusken C, Koopmans MP, Drosten C.**
461 2020. Detection of 2019 novel coronavirus (2019-nCoV) by real-time RT-PCR. *Euro Surveill* **25**.
- 462 11. **Rahmani AR, Leili M, Azarian G, Poormohammadi A.** 2020. Sampling and detection of corona
463 viruses in air: A mini review. *Sci Total Environ* **740**:140207.
- 464 12. **Matsuyama S, Nao N, Shirato K, Kawase M, Saito S, Takayama I, Nagata N, Sekizuka T, Katoh H,**
465 **Kato F, Sakata M, Tahara M, Kutsuna S, Ohmagari N, Kuroda M, Suzuki T, Kageyama T, Takeda M.**
466 2020. Enhanced isolation of SARS-CoV-2 by TMPRSS2-expressing cells. *Proc Natl Acad Sci U S A*
467 **117**:7001-7003.
- 468 13. **van Doremalen N, Bushmaker T, Morris DH, Holbrook MG, Gamble A, Williamson BN, Tamin A,**
469 **Harcourt JL, Thornburg NJ, Gerber SI, Lloyd-Smith JO, de Wit E, Munster VJ.** 2020. Aerosol and
470 Surface Stability of SARS-CoV-2 as Compared with SARS-CoV-1. *N Engl J Med* **382**:1564-1567.
- 471 14. **Aganovic A, Bi Y, Cao G, Drangsholt F, Kurnitski J, Wargocki P.** 2021. Estimating the impact of indoor
472 relative humidity on SARS-CoV-2 airborne transmission risk using a new modification of the Wells-
473 Riley model. *Build Environ* **205**:108278.
- 474 15. [https://www.rehva.eu/fileadmin/content/documents/Downloadable_documents/REHVA_COVID-](https://www.rehva.eu/fileadmin/content/documents/Downloadable_documents/REHVA_COVID-19_Ventilation_Calculator_user_guide_V2.0.pdf)
475 [19_Ventilation_Calculator_user_guide_V2.0.pdf](https://www.rehva.eu/fileadmin/content/documents/Downloadable_documents/REHVA_COVID-19_Ventilation_Calculator_user_guide_V2.0.pdf).
- 476 16. **Buonanno G, Morawska L, Stabile L.** 2020. Quantitative assessment of the risk of airborne
477 transmission of SARS-CoV-2 infection: Prospective and retrospective applications. *Environ Int*
478 **145**:106112.
- 479 17. [https://pusprajbhatt.files.wordpress.com/2017/12/india-national-building-code-nbc-2016-vol-](https://pusprajbhatt.files.wordpress.com/2017/12/india-national-building-code-nbc-2016-vol-2.pdf)
480 [2.pdf](https://pusprajbhatt.files.wordpress.com/2017/12/india-national-building-code-nbc-2016-vol-2.pdf).
- 481 18. **Diapouli E, Chaloulakou A, Koutrakis P.** 2013. Estimating the concentration of indoor particles of
482 outdoor origin: a review. *J Air Waste Manag Assoc* **63**:1113-1129.
- 483 19. [https://indico.fnal.gov/event/10650/attachments/3160/3783/ParticleDepositionRates_Thatcher_et](https://indico.fnal.gov/event/10650/attachments/3160/3783/ParticleDepositionRates_Thatcher_et_al_2002.pdf)
484 [_al_2002.pdf](https://indico.fnal.gov/event/10650/attachments/3160/3783/ParticleDepositionRates_Thatcher_et_al_2002.pdf).
- 485 20. **Fears AC, Klimstra WB, Duprex P, Hartman A, Weaver SC, Plante KC, Mirchandani D, Plante JA,**
486 **Aguilar PV, Fernandez D, Nalca A, Totura A, Dyer D, Kearney B, Lackemeyer M, Bohannon JK,**
487 **Johnson R, Garry RF, Reed DS, Roy CJ.** 2020. Comparative dynamic aerosol efficiencies of three
488 emergent coronaviruses and the unusual persistence of SARS-CoV-2 in aerosol suspensions.
489 medRxiv doi:10.1101/2020.04.13.20063784.
- 490 21. **Harcourt J, Tamin A, Lu X, Kamili S, Sakthivel SK, Murray J, Queen K, Tao Y, Paden CR, Zhang J, Li**
491 **Y, Uehara A, Wang H, Goldsmith C, Bullock HA, Wang L, Whitaker B, Lynch B, Gautam R,**
492 **Schindewolf C, Lokugamage KG, Scharton D, Plante JA, Mirchandani D, Widen SG, Narayanan K,**
493 **Makino S, Ksiazek TG, Plante KS, Weaver SC, Lindstrom S, Tong S, Menachery VD, Thornburg NJ.**
494 2020. Severe Acute Respiratory Syndrome Coronavirus 2 from Patient with Coronavirus Disease,
495 United States. *Emerg Infect Dis* **26**:1266-1273.
- 496 22. **Jain A, Grover V, Singh C, Sharma A, Das DK, Singh P, Thakur KG, Ringe RP.** 2021. Chlorhexidine:
497 An effective anticovid mouth rinse. *J Indian Soc Periodontol* **25**:86-88.
- 498 23. **Setlow RB, Setlow JK.** 1962. Evidence that ultraviolet-induced thymine dimers in DNA cause
499 biological damage. *Proc Natl Acad Sci U S A* **48**:1250-1257.

- 500 24. **Goes LR, Siqueira JD, Garrido MM, Alves BM, Pereira A, Cicala C, Arthos J, Viola JPB, Soares MA,**
501 **Force IC-T.** 2021. New infections by SARS-CoV-2 variants of concern after natural infections and
502 post-vaccination in Rio de Janeiro, Brazil. *Infect Genet Evol* **94**:104998.
- 503 25. **Mizrahi B, Lotan R, Kalkstein N, Peretz A, Perez G, Ben-Tov A, Chodick G, Gazit S, Patalon T.** 2021.
504 Correlation of SARS-CoV-2-breakthrough infections to time-from-vaccine. *Nat Commun* **12**:6379.
- 505